Evaluation of Aspects of E^* Test by Using Hot-Mix Asphalt Specimens with Varying Void Contents

Geoffrey M. Rowe, Salman Hakimzadeh Khoee, Phillip Blankenship, and Kamyar C. Mahboub

A dynamic modulus master curve for asphalt concrete is a critical input for flexible pavement design in the Mechanistic–Empirical Pavement Design Guide developed in NCHRP Project 1-37A, which has drawn much attention among asphalt technologists. The objectives in this study were (*a*) to consider and compare different analysis techniques for construction of the master curve and (*b*) to measure and analyze the effect of permanent strain on samples that have been evaluated with one of the simple performance tests, dynamic modulus. It was found that differences existed in the calculated asymptote values and the shape of the master curve, depending upon which method was adopted. Recommendations are made for modifications to the testing protocol and for further work to determine the effect of permanent strain at higher test temperatures.

The dynamic modulus of an asphalt mixture is a significant parameter that determines the ability of a material to resist compressive deformation as it is subjected to cyclic compressive loading and unloading. The dynamic modulus test has been suggested by NCHRP Projects 9-19 and 9-29 as a simple performance test (SPT) to verify the performance characteristics of Superpave® mixture designs (*1*). It has also been suggested as the potential quality control–quality assurance parameter in the field (*2*). Dynamic modulus is also an input to the Mechanistic–Empirical Pavement Design Guide (MEPDG) (*3*) and supports the predictive performance models developed as part of NCHRP project 1-37A (*4*).

For viscoelastic materials such as hot-mix asphalt mixtures, the stress–strain relationship under a continuous sinusoidal loading is defined by its complex dynamic modulus (E^*). This is a complex number that relates stress to strain for linear viscoelastic materials subjected to continuously applied sinusoidal loading in the frequency domain. The complex modulus is defined as the ratio of the amplitude of the sinusoidal stress to the amplitude of the sinusoidal strain, as follows:

$$|E^*| = \frac{\sigma}{\epsilon}$$

where σ is the amplitude of stress and ϵ is the amplitude of strain.

G. M. Rowe, Abatech, Inc., P.O. Box 356, Blooming Glen, PA 18911. S. Hakimzadeh Khoee and K. C. Mahboub, University of Kentucky, 161 Oliver Raymond Building, Lexington, KY 40506-0281. P. Blankenship, Asphalt Institute, 2696 Research Park Drive, Lexington, KY 40511. Corresponding author: S. Hakimzadeh Khoee, hakimza1@uiuc.edu.

Transportation Research Record: Journal of the Transportation Research Board, No. 2127, Transportation Research Board of the National Academies, Washington, D.C., 2009, pp. 164–172.
DOI: 10.3141/2127-19

In addition, the lag between the load and the deformation signal, expressed as a phase angle (ϕ), is further related to the complex modulus as follows:

$$|E^*| = \left[E'^2 + E''^2\right]^{0.5}$$

where E' = storage modulus ($|E^*| \cos \phi$) and E'' = loss modulus ($|E^*| \sin \phi$).

For a pure elastic material, $\phi = 0$, whereas for a pure viscous material, $\phi = 90°$. Typical values of ϕ for most asphalt mixtures range from 0° to 60°. The testing of dynamic modulus of asphalt mixtures has shown that generally a viscoelastic solid model best describes the performance over a wide range of frequencies and temperatures, with the dynamic modulus expressed as a sigmoid function. In this type of model, the phase lag typically will vary from 0° to approximately 60°.

SAMPLE PREPARING AND LABORATORY TESTING

Seven sets of specimens (a total of 14 specimens, with two replicates per set) were used in this study. The materials being evaluated were made with a series of void contents and were referenced as 1 to 7, with 1 corresponding to the highest void content and 7 corresponding to the lowest. All work was performed at the Asphalt Institute, Lexington, Kentucky.

A standard Kentucky job mix formula was blended with 5.4% asphalt binder. The aggregate composition was 25% limestone #8s, 26% limestone sand (unwashed), 14% limestone sand (washed), and 15% natural sand (rounded). The asphalt binder that was used in this study (PG 64-22) was from a local terminal and is used widely in Kentucky. The gravities for the aggregate, G_b, G_{sb}, and G_{se}, were 1.030, 2.68, and 2.724, respectively. The asphalt binder content of 5.4% was optimized by using a Superpave 9.5-mm coarse-graded mixture design at 75 gyrations and 4.0% air voids.

To fabricate the specimens with different air void levels, the quantity of the materials used to prepare the specimens was varied and a standard compaction height was used. The aggregates and asphalt were mixed and aged according to AASHTO R30, Mixture Conditioning of Hot-Mix Asphalt (Section 7.2, Short-Term Conditioning for Mixture Mechanical Property Testing). The aging and compaction temperature was 135°C (275°F). The mixture was placed into the Superpave gyratory compactor (SGC) and set to a 150-mm compaction height. The volumetrics of the materials are summarized in Table 1. The target air voids for each set was at an increment of

TABLE 1 Compacted Volumetric Characteristics

Series Ref.	Air Voids (%)	Voids in Mineral Aggregate (%)	Voids Filled with Asphalt (%)
1	11.3	21.1	46.3
2	9.8	19.8	50.2
3	8.4	18.5	54.6
4	7.1	17.4	58.8
5	5.5	15.9	65.4
6	3.8	14.5	73.4
7	2.3	13.1	82.1

NOTE: Ref. = reference.

1.5% ± 0.3%. The average values of each set are reported throughout this paper.

The $|E^*|$ tests were performed for the seven series (14 specimens, two at each void content) at three temperatures (4°C, 20°C, and 40°C) and with nine frequencies (25, 20, 10, 5, 2, 1, 0.5, 0.2, 0.1 Hz), which are in accordance with AASHTO TP 62-03. The $|E^*|$ for each test condition was determined through the use of the average amplitude of the haversine load from the load cell and the average deformation measured from each axial linear variable differential transformer. Details on computation of $|E^*|$ are provided in NCHRP Report 465 (*5*).

DATA ANALYSIS

In the proposed 2002 Guide for the Design of Pavement Systems, the modulus of the asphalt concrete is determined from a master curve constructed at a reference temperature. Master curves are constructed by using the principle of time–temperature superposition (Figure 1). The data at various temperatures should be shifted with respect to the log of time until the curves merge into a single smooth function. The resulting master curve of the modulus as a function of time formed in this manner describes the time dependency of the material. The amount of shift required at each temperature to form the master curve describes the temperature dependency of the material. The master curve within the MEPDG is of a standard sigmoid form, which is referenced as Witczak's (symmetrical or standard logistic) sigmoid, as follows:

$$\log|E^*| = \delta + \frac{\alpha}{1 + e^{\beta+\gamma(\log\omega)}}$$

where

δ = lower asymptote, limit for $|E^*|$ at long loading times and high temperatures,
α = describes upper asymptote [$(\delta + \alpha)$ gives limit for $|E^*|$ at short loading times and low temperatures],
ω = frequency (Hz), and
β and γ = shape of sigmoid.

An alternative sigmoid that can be used is the Richards (nonsymmetrical or generalized logistic) sigmoid (*6*).

$$\log|E^*| = \delta + \frac{\alpha}{\left[1 + e^{\beta+\gamma(\log\omega)}\right]^{\frac{1}{\lambda}}}$$

where β, γ, and λ define the shape of the sigmoid.

The principle advantage of Richards' equation over the standard logistic is that greater flexibility exists in fitting nonsymmetric master curve data. The nonsymmetric behavior is evidenced by an inflection point that is not half the distance between the maximum and minimum dynamic complex moduli.

Data have been analyzed by using several procedures, as follows:

1. Microsoft Excel Solver analysis was used to obtain master curve fits by means of the Witczak sigmoid function.
2. RHEA, developed by Rowe and Sharrock (*7*), was used to produce an analysis with discrete spectra to obtain glassy and equilibrium modulus values and other contributing parameters to the relaxation and retardation spectra.
3. RHEA was further used to determine fits to both Witczak's sigmoid (standard logistic curve) and Richards' sigmoid (generalized logistic curve) functions.

The glassy and equilibrium moduli are considered the asymptotes that are obtained from the various model fits with the glassy modulus corresponding to the higher asymptote and the equilibrium modulus corresponding to the lower asymptote. The values can also be obtained from the fit of a relaxation spectrum or retardation spectrum for a viscoelastic solid model. In the analysis, these parameters have been computed from all three methods that have been defined and presented for comparison.

The parameters associated with the above analysis have all been prepared for a reference temperature of 20°C. In the analysis of data

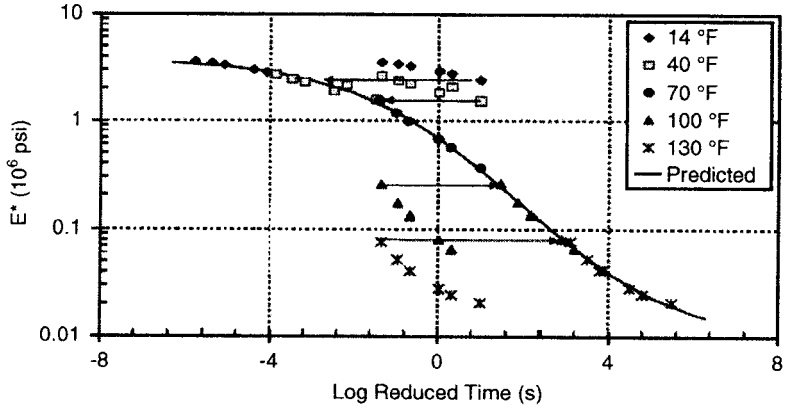

FIGURE 1 Example of master curve construction in reduced-time format (time taken to be seconds = 1/frequency) [from ARA (*3*)].

TABLE 2 Witczak Parameters Computed Using Excel and Solver

Series Ref.	ΔE_a	δ	β	γ	Max. Glassy Modulus (MPa)	Equilibrium Modulus (MPa)	Inflection Point (Hz)
1	232,015.5	−7.31	−2.63	−0.34	20,063.12	0.0395167	1.34E-05
2	225,562.7	−3.97	−2.21	−0.37	23,058.85	0.0538788	1.77E-05
3	214,221	−0.85	−1.62	−0.43	26,278.45	0.0484777	1.36E-05
4	206,281.1	−0.15	−1.53	−0.50	34,241.09	0.0035881	2.08E-06
5	205,799.3	−0.24	−1.56	−0.48	28,776.23	0.2062729	3.95E-05
6	201,568.5	0.37	−1.48	−0.55	36,696.7	0.047569	9.57E-06
7	200,586.6	0.7	−1.42	−0.57	39,042.9	0.051995	6.88E-06

in the RHEA software, the shifting was performed by using the Gordon and Shaw (8) procedures, whereas with the Excel program with Solver, the fitting was done by numerical optimization to the Witczak symmetrical sigmoid model.

ANALYSIS RESULTS

In the Excel Solver analysis, the general form of the dynamic modulus master curve was a modified version of the dynamic modulus master curve equation included in the MEPDG (AASHTO TP62-03):

$$\log|E^*| = \delta + \frac{(\max - \delta)}{1 + e^{\beta + \gamma(\log \omega_r)}}$$

where

ω_r = reduced frequency (Hz),
max = limiting maximum modulus (at the glassy condition, psi), and
β, δ, and γ = fitting parameters.

The shift factors at each temperature are given by

$$\log a(t) = \frac{\Delta E_a}{19.147\left(\frac{1}{T} - \frac{1}{T_r}\right)}$$

where

$a(t)$ = shift factor at temperature T,
T_r = reference temperature (K),
T = test temperature (K), and
ΔE_a = activation energy.

With the use of this model and Mastersolver, Version 2.0, developed by NCHRP (2), the Witczak parameters and master curves for different air voids were obtained, as shown in Table 2 and Figure 2. The information plotted in Figure 2 has been plotted with a log-normal graph to demonstrate the differences in dynamic modulus at the high end of the scale.

In the RHEA analysis, results were obtained for the glassy and equilibrium moduli from the fitting of a discrete spectra (or Prony

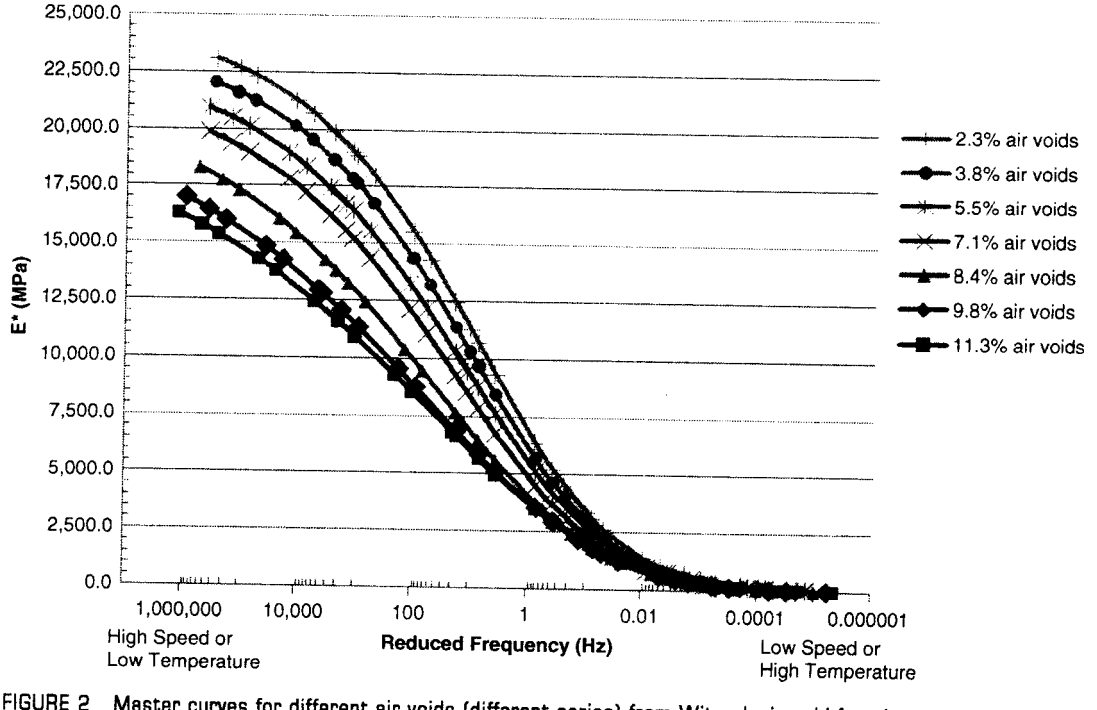

FIGURE 2 Master curves for different air voids (different series) from Witczak sigmoid function.

TABLE 3 Equilibrium Dynamic Modulus (E_e), Glassy Dynamic Compliance (D_g), and Glassy Dynamic Modulus (E_g)

Series Ref.	E_e (MPa)	D_g (1/MPa)	E_g (MPa)
1	6.74E-01	5.83E-05	1.72E+04
2	4.28E+00	5.50E-05	1.82E+04
3	9.63E+00	5.10E-05	1.96E+04
4	1.57E-01	3.87E-05	2.59E+04
5	3.34E+01	4.25E-05	2.35E+04
6	4.73E+01	3.57E-05	2.80E+04
7	2.74E+01	3.16E-05	3.16E+04

series) (Table 3). In addition, the results are presented for the two sigmoid formats discussed earlier for the Witczak sigmoid in Table 4, whereas the parameters for the Richards model are given in Table 5.

DISCUSSION OF RESULTS

Glassy Modulus

The complex modulus at the glassy condition was analyzed through various methods as described earlier. In addition, the aggregate gradation and mixture volumetrics have also been used to determine this parameter. The analysis for three of the cases is illustrated in (Figure 3) for three methods of analysis versus the prediction method. These data suggest that the MEPDG prediction procedure significantly overpredicts the glassy asymptote. The one data point above the line of equality was for a result that was more difficult to analyze and involved some software modifications for the analysis. The Excel Solver and the logistic models in RHEA tended to produce similar results for the glassy asymptote. The discrete spectrum appears to produce a lower analysis number than the other methods, which can be partly expected because this is an extremely significant analysis method compared with the functional fitting methods.

The effect of air voids on the glassy modulus is clearly illustrated in Figure 4. The air voids appear to be the best volumetric parameter to describe the variation in the glassy asymptote. However, additional studies may suggest other important volumetric parameters affecting this value.

Equilibrium Modulus

The value of the equilibrium modulus obtained from the different analysis methods differs widely. The ranges obtained are shown in Table 6. The values obtained trend in general agreement with the air void contents. The lowest values were obtained by using the Excel with the Solver analysis procedure, whereas the highest values were obtained from the data analysis by using the RHEA software and Richards' equation. The values from RHEA by using the Witczak equation (standard-logistic) give numerical values below those developed from the predictive equation. All the analysis techniques showed more sensitivity to air void level than the predictive equation developed by Witczak, as illustrated in Figure 5.

The analysis that gave values closest to those predicted from the Witczak predictive approach was the RHEA sigmoid analysis method. However, the numerical procedures used to fit the Richards sigmoid require some modifications. The standard sigmoid is a special case of the generalized sigmoid, where $\lambda = 1$, as shown by Rowe et al. (9). A significant amount of extrapolation in the data occurred to define

TABLE 4 Witczak Parameters Computed with RHEA Software

Series Ref.	α	δ	β	γ	Glassy Modulus (MPa)	Equilibrium Modulus (MPa)	Inflection Point (Hz)
1	5.253229	−0.9545273	−1.723188563	−0.3829005	19,893	0.111	3.16E-05
2	4.612674	−0.2491132	−1.641044545	−0.42797	23,097	0.563	1.46E-04
3	3.998142	0.3805879	−1.45154412	−0.4421184	23,918	2.402	5.21E-04
4	5.021598	−0.5319336	−1.590735017	−0.3775729	30,879	0.294	6.12E-05
5	4.193462	0.2361922	−1.555829066	−0.4370865	26,894	1.723	2.76E-04
6	4.168391	0.3567095	−1.521166826	−0.4294803	33,504	2.274	2.87E-04
7	3.980174	0.5470085	−1.515648532	−0.4312255	33,665	3.524	3.06E-04

TABLE 5 Richards Parameters for Dynamic Modulus Mastercurve

Series Ref.	α	δ	β	γ	λ	Glassy Modulus (MPa)	Equilibrium Modulus (MPa)	Inflection Point (Hz)
1	4.284639	0.0856861	−1.6263765	−0.36139	0.0269762	23,460	1.218	3.16E-05
2	4.094	0.301216	−1.5136863	−0.39476	0.3657426	24,844	2.001	1.46E-04
3	3.871488	0.5072934	−1.4245677	−0.4339	0.8406166	23,921	3.216	5.21E-04
4	3.406716	1.239363	−1.1996798	−0.28475	0.6532455	44,267	17.353	6.12E-05
5	2.963827	1.5033	−1.2466533	−0.42988	0.001	29,318	31.864	1.26E-03
6	2.932582	1.619395	−1.2307169	−0.42931	0.001	35,643	41.629	1.36E-03
7	3.314477	1.252753	−1.336007	−0.38011	0.088893	36,917	17.896	3.06E-04

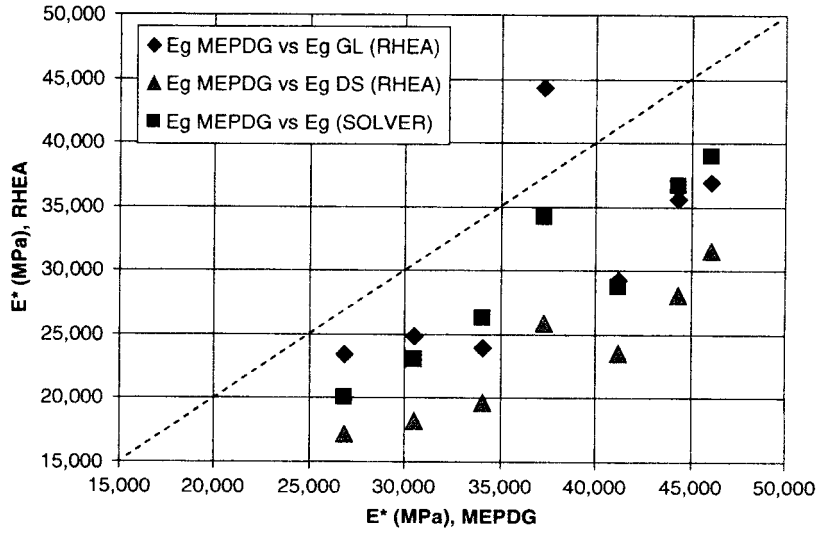

FIGURE 3 Glassy modulus from MEPDG prediction equation that used mixture properties versus glassy modulus from test data computed with RHEA (GL = generalized logistic function, DS = discrete spectra) and Solver (from Excel).

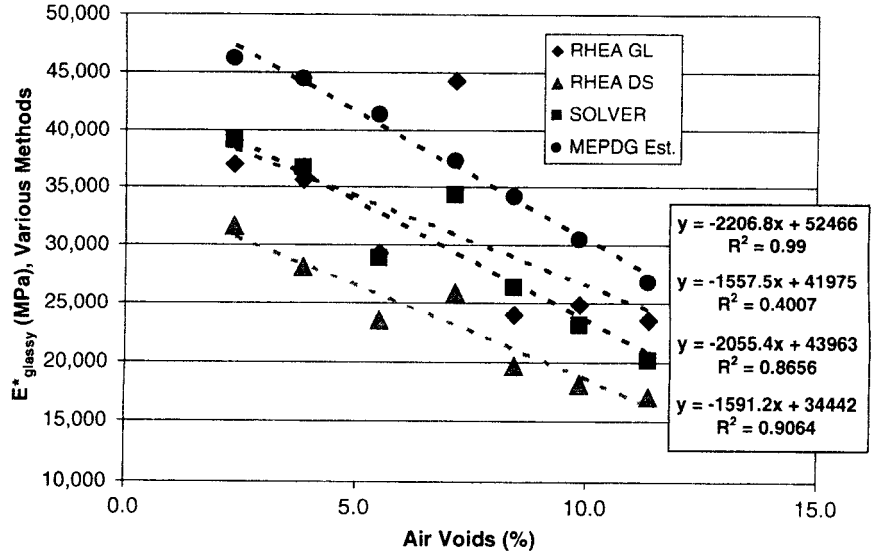

FIGURE 4 Effect of air voids on glassy asymptote equilibrium modulus.

TABLE 6 Equilibrium Modulus Ranges and Average from Various Methods

	Equilibrium Modulus (MPa)		
Analysis Method	Low Value	High Value	Average
RHEA DS	0.674	47.323	19.765
RHEA GL	1.218	41.629	16.454
RHEA SL	0.111	3.524	1.556
EXCEL with SOLVER	0.004	.206	0.067
Witczak predication	3.9	6.7	5.443

NOTE: DS = discrete spectra, GL = generalized logistic curve function, and SL = standard logistic curve function.

the full sigmoid parameters with all three approaches. Typically, the data covered 2½ decades of stiffness, whereas the prediction models defined approximately five decades of stiffness. The data defined more closely the low-temperature properties, whereas the more-significant extrapolation by the models was taking place at the high-temperature end of the testing.

The data obtained at the highest test temperature were not fitting the expected phase-angle relationship as calculated from the differential of the master curve model form (*10*), as shown in Figure 6. This finding led to some investigative analysis of the cause of this difference. Testing revealed that some permanent deformation of the specimens was taking place, and this appears to be related to the void level in the specimen, as observed in Figure 7. The difference in air voids before and after the $|E^*|$ test was negligible, as shown in

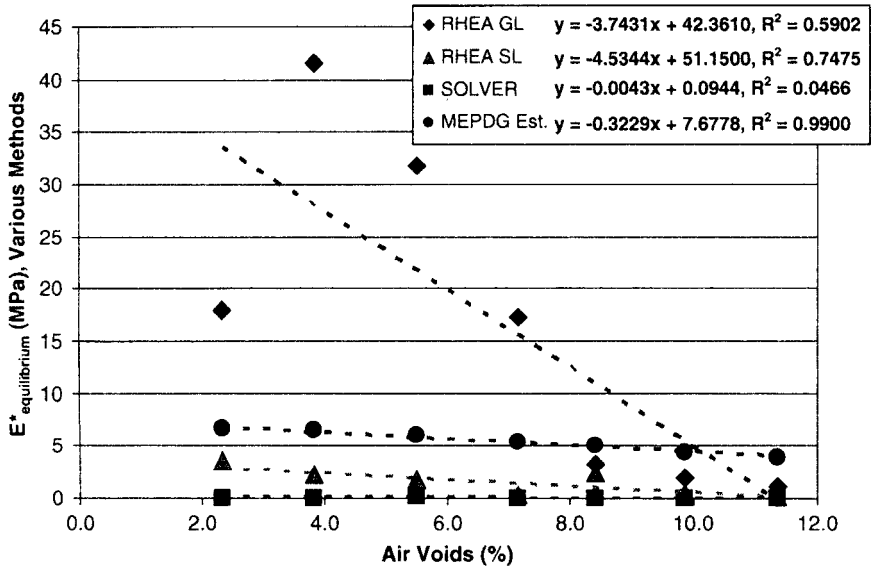

FIGURE 5 Values of equilibrium modulus versus air void content.

Figure 8, and was the value of modulus when remeasured at 20°C (Figure 9). The deformation that occurred in the specimen during high-temperature testing (40°C) was clearly evident through inspection of Figures 10 through 12. This example shows that, from the tests at 25 to 2 Hz, the specimen had deformed by approximately 600 μstrain. The data then appear to show recovery of the specimen, although this is not physically possible with the haversine loading—and additional permanent deformation must be occurring. The apparent recovery was most likely associated with software issues, numerical issues, or both, and is currently being investigated. The specimen was most likely experiencing further deformation consistent with the data in Figure 7, which suggest a permanent strain approaching 1,500 μstrain. This level of strain during the $|E^*|$ test most likely resulted in nonlinear behavior and deviation of the phase angle response from the expected behavior. Due to the high permanent strain on the modulus samples, they should not be used for flow number testing. New samples that have not been deformed should be used for flow number testing.

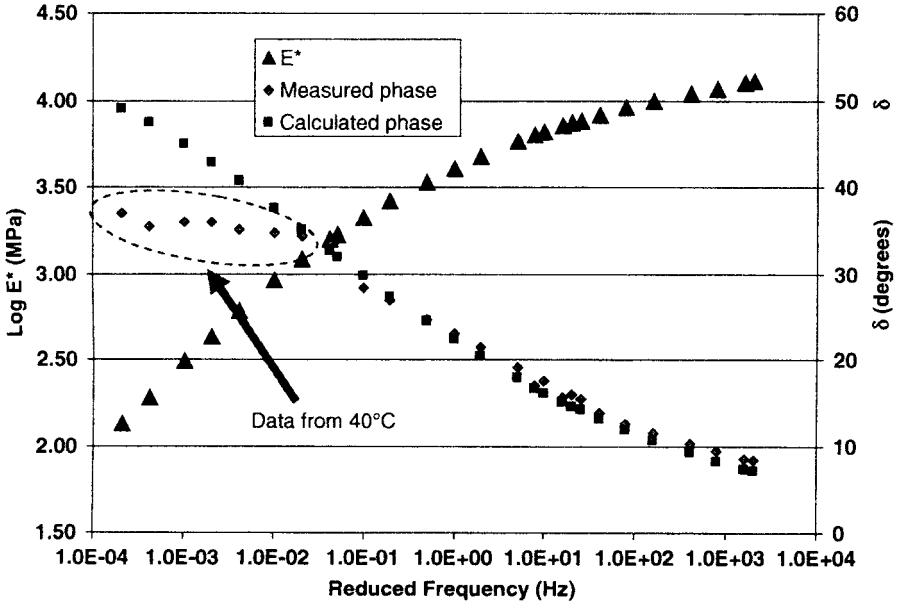

FIGURE 6 Differences in observed and calculated phase angle with the procedure developed by Rowe (*10*) observed in all materials, with divergent data for the 40°C isotherm (reference temperature (T_{ref}) = 20°C).

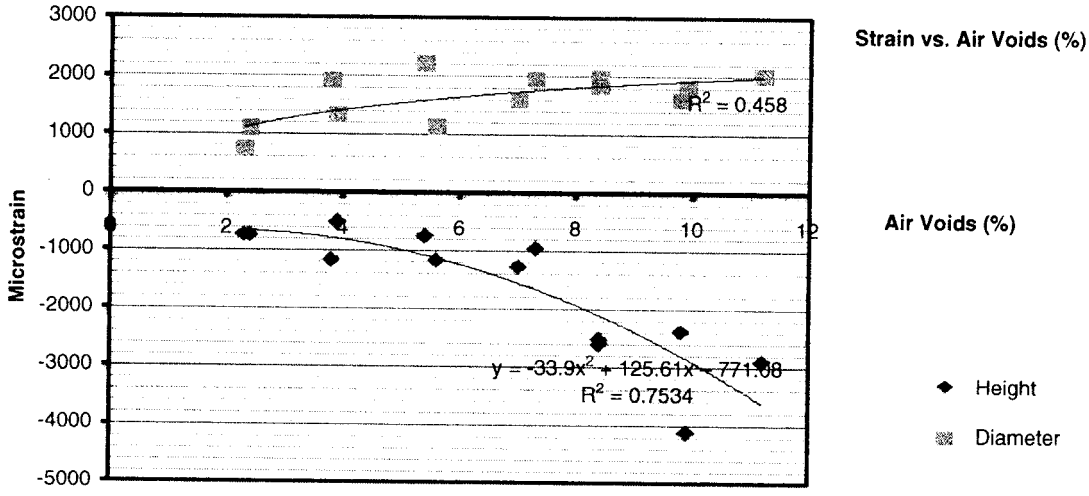

FIGURE 7 Permanent strains in specimens versus air voids (after SPT test).

CONCLUSIONS

The results of this analysis lead to the following observations:

1. The values of equilibrium and glassy moduli are significantly affected by the selected analysis method as well as by the volumetric properties of the mixture.
2. The MEPDG prediction procedure significantly overpredicts the glassy asymptote.
3. The phase analysis data obtained from the high-temperature testing did not coincide with the expected relationship for this parameter. It is highly likely that large permanent strain was significantly affecting this parameter.
4. Retests of material properties at 20°C before and after the full frequency sweep data gave quite similar results.
5. The permanent strain occurring in any given specimen appeared to be significantly affected by the volumetrics. Additional work is required to deduce whether this is truly a volumetric effect or a stiffness effect.
6. Dynamic modulus samples that incur this large permanent strain should not be used for further testing. New samples should be made for flow number testing.

The work presented in this paper is limited to one mixture type, one binder type, and content. Consequently, care should be taken when these data are applied to other materials. Additional work is recommended to improve the understanding of the causes and effects reported in this paper.

ACKNOWLEDGMENTS

The authors gratefully acknowledge the support of the Kentucky Transportation Cabinet and the Federal Highway Administration for funding this study. They also thank the University of Kentucky

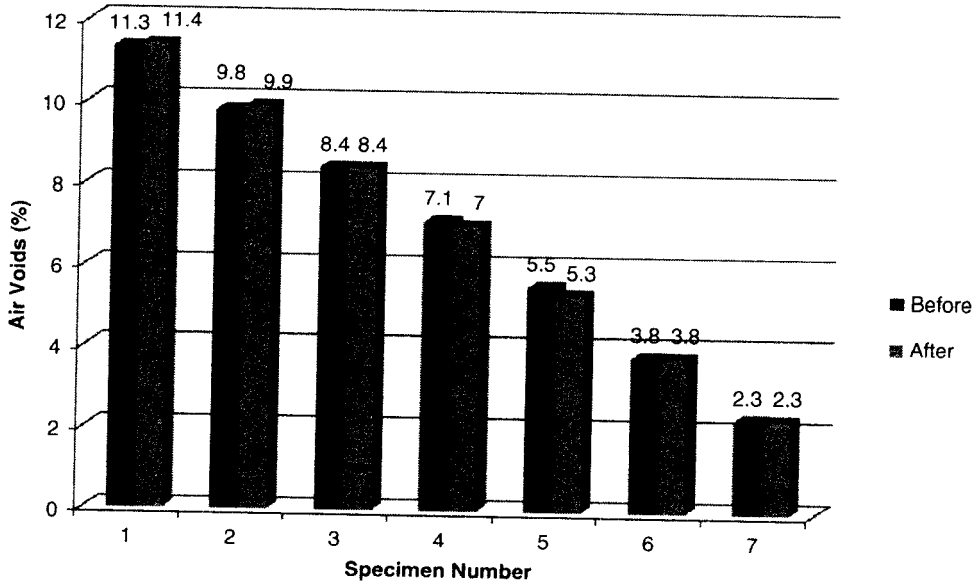

FIGURE 8 Comparison of air voids of specimens before and after E^* test.

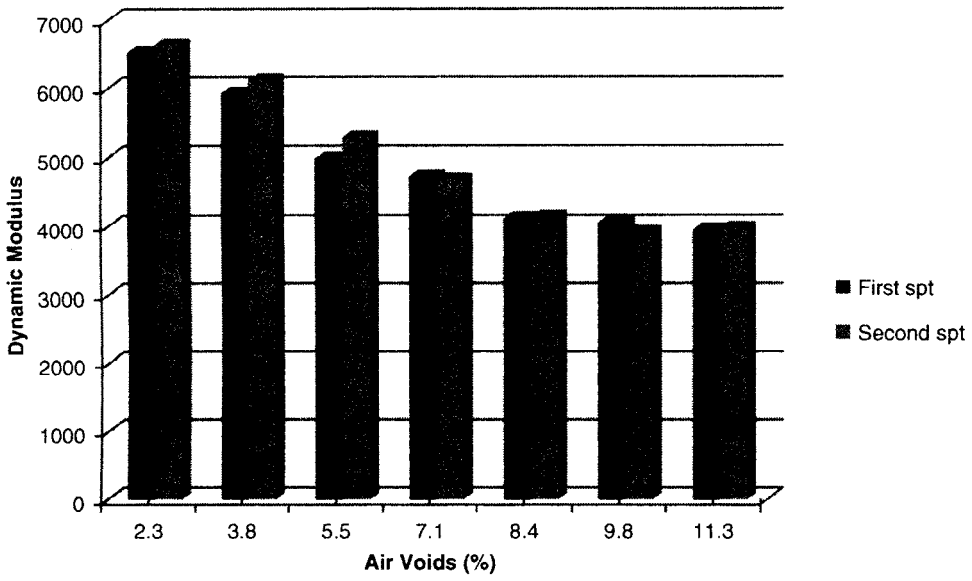

FIGURE 9 Effect of permanent strain on samples in SPT modulus test (conducted at 1 Hz and 20°C).

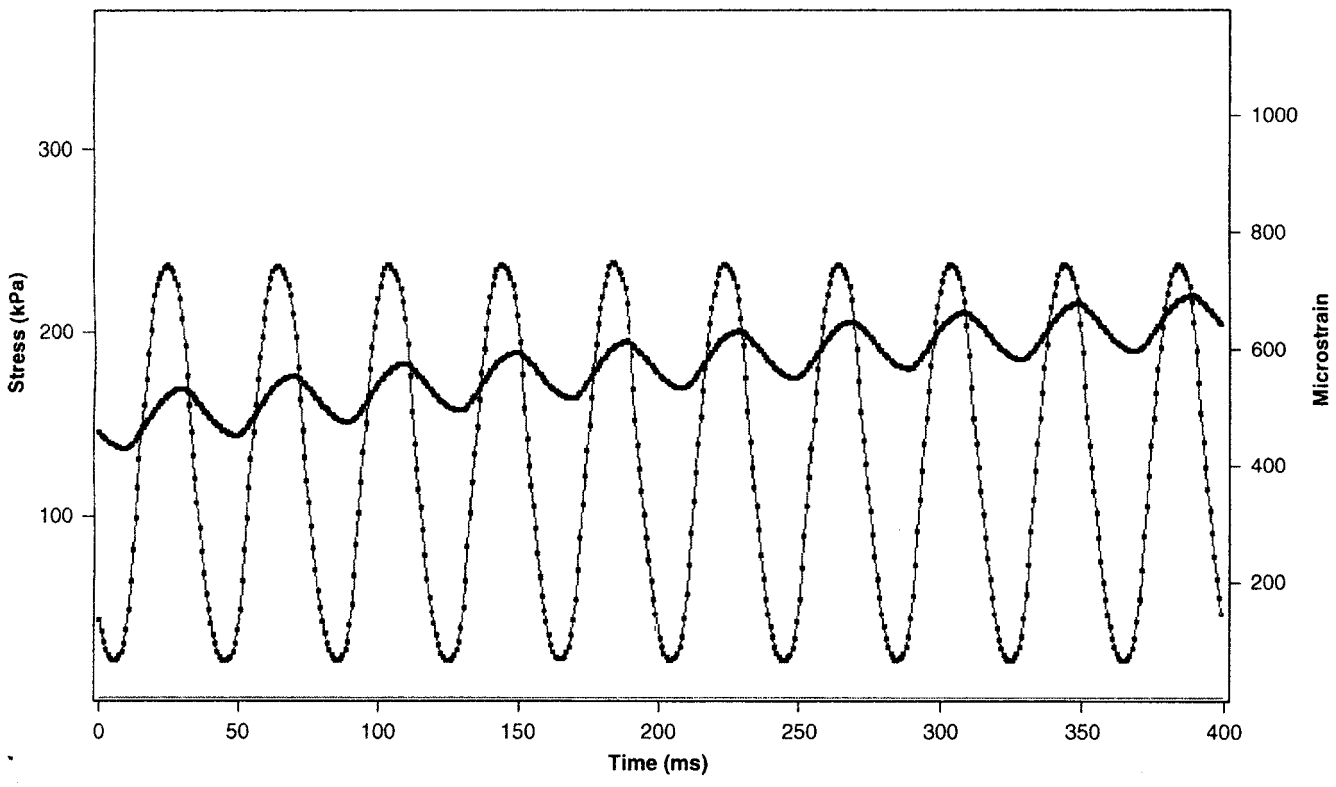

FIGURE 10 Example of creep in experimental data, Specimen 7*b* (25 Hz and 40°C).

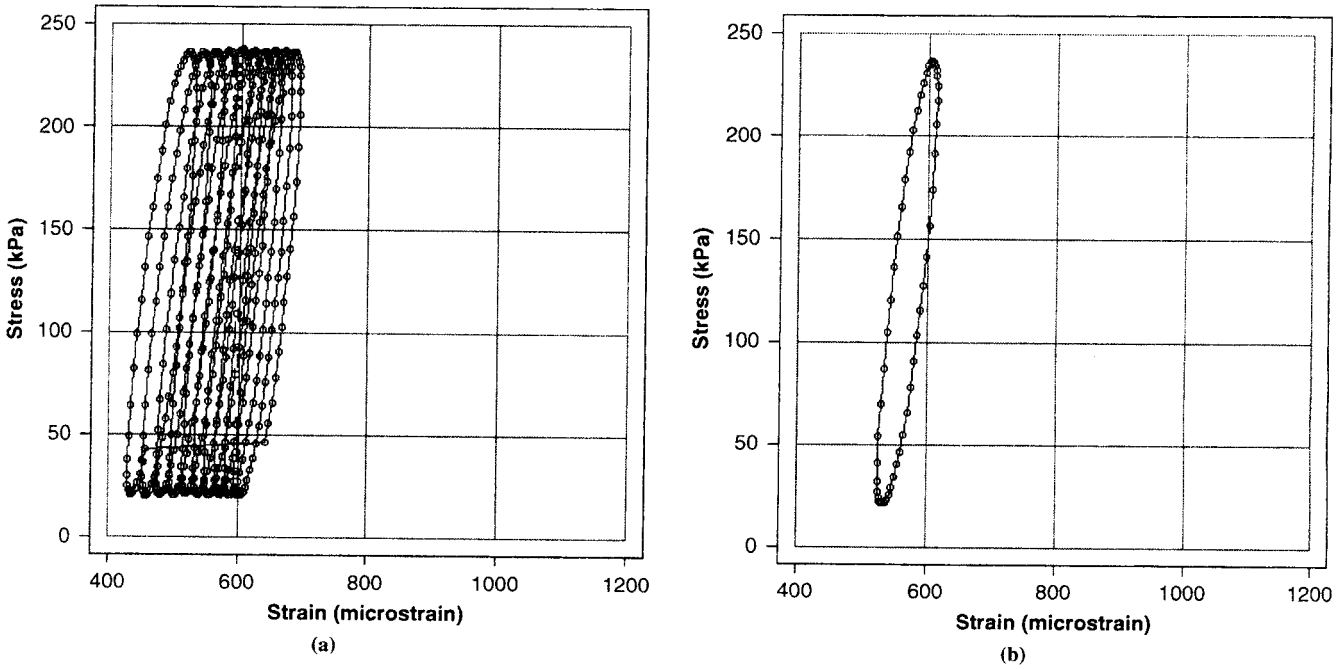

FIGURE 11 Data from (*a*) total hysteresis used to produce (*b*) average hysteresis loop for clarity in observing variation of stress and strain during test.

Transportation Center, the prime contractor of this research. The authors thank the staff at the Asphalt Institute, especially Shay Emmons and Jason Coleman, for their help in preparing the study specimens. The authors also thank Clark Graves of the University of Kentucky for his help in this study and Mark Sharrock of Abatech International, Ltd., for conducting analyses. Each of these colleagues played a vital role in this work.

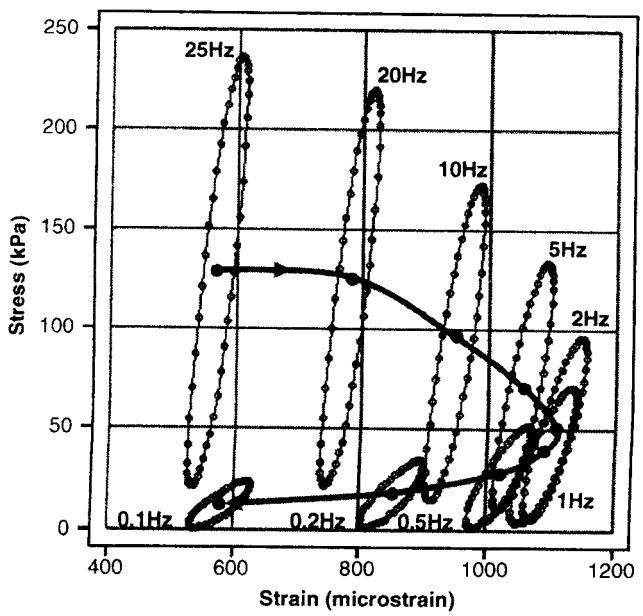

FIGURE 12 Variation in position of mean hysteresis loop as reported by software for SPT test, Specimen 7*b* (40°C).

REFERENCES

1. Witczak, M. W., and T. K. Pellinen. AC Mixture Response Comparison to Performance $|E^*|$ and Sm Prediction Equation Methodology Results. *Superpave Support and Performance Models Management, Task C: Simple Performance Test. NCHRP Project 9-19.* Team Report SPT-ALF-2(L). TRB, National Research Council, Washington, D.C., 2000.
2. Bonaquist, R. F. *Simple Performance Tester for Superpave Mix Design.* Quarterly Progress Report, NCHRP Project 9-29, Transportation Research Board of the National Academies, Washington, D.C., 2003.
3. ARA, Inc., ERES Consultants Division. *Guide for Mechanistic–Empirical Design of New and Rehabilitated Pavement Structures.* Final report, NCHRP Project 1-37A. Transportation Research Board of the National Academies, Washington, D.C., 2004. www.trb.org/mepdg/guide.htm.
4. Witczak, M. *NCHRP Report 547: Simple Performance Tests: Summary of Recommended Methods and Database.* Transportation Research Board of the National Academies, Washington, D.C., 2005.
5. Witczak, M. W., K. Kaloush, T. Pellinen, M. El-Basyouny, and H. Von Quintus. *NCHRP Report 465: Simple Performance Test for Superpave Mix Design.* TRB, National Research Council, Washington, D.C., 2002.
6. Richards, F. J. A Flexible Growth Function for Empirical Use. *Journal of Experimental Botany,* Vol. 10, No 29, 1959, pp. 290–300.
7. Rowe, G. M., and M. J. Sharrock. Development of Standard Techniques for the Calculation of Master Curves for Linear-Visco Elastic Materials. Presented at 1st International Symposium on Binder Rheology and Pavement Performance. University of Calgary, Alberta, Canada, August 14–15, 2000.
8. Gordon, G. V., and M. T. Shaw. *Computer Programs for Rheologists.* Hanser–Gardner Publications, Cincinnati, Ohio, 1994.
9. Rowe, G. M., G. Baumgardner, and M. J. Sharrock. A Generalized Logistic Function to Describe the Master Curve Stiffness Properties of Binder Mastics and Mixtures. Presented at 45th Petersen Asphalt Research Conference, University of Wyoming, Laramie, July 14–16, 2008.
10. Rowe, G. M. Phase Angle Determination and Interrelationships Within Bituminous Materials. Presented at 45th Petersen Asphalt Research Conference, University of Wyoming, Laramie, July 14–16, 2008.

The Characteristics of Bituminous Paving Mixtures to Meet Structural Requirements Committee sponsored publication of this paper.